Field line tying and magnetic shear effects of the vertical magnetic field on low frequency density fluctuations in CPD

Tomofumi RYOUKAI[1)], Hideki ZUSHI[2)], Rajendraprasad BHATTACHARYAY[1)], Hiroshi IDEI[2)], Tomokazu YOSHINAGA[3)], CPD Group1[2)], Tomohiro MORISAKI[3)], Takashi MUTOH[3)], Shin KUBO[3)], Kazuaki NAGASAKI[4)]

1)Interdisciplinary Graduate School of Engineering Science, Kyushu University Kasuga, Fukuoka 816-8580, Japan, 2)RIAM, Kyushu University, 3)NIFS, 322-6 Oroshi, Toki, Gifu 50-5292, 4)Kyoto University Kyoto

(Received: 19 September 2008 / Accepted: 25 February 2009)

The two dimensional structure of density fluctuations is examined in a microwave produced annulus plasma at B_t = 0.3 T. In simple torus configuration low frequency coherent waves are found to be unstable and the density fluctuation level reaches to 30-40 %. By applying B_z field (50 G) it should be noted that the fluctuation level is reduced by 80 % and no coherent modes are found. The current ramp-up condition is discussed from a view point of the improved mode conversion of incident cyclotron waves with reduced fluctuations.

Keywords: non-inductive current drive, low frequency density fluctuations, EBW, ECW, Li sheet beam

1. Introduction

In the spherical tokamak device CPD (Compact Plasma wall interaction experimental Device), the non-inductive current drive experiments have been performed in hydrogen plasma using electron cyclotron waves [1]. At 1 kW of the rf power at 8.2 GHz an annulus plasma is initially produced near the resonance layer R_{res} (~0.16 - 0.19 m) and is extended radially up to ~ 0.1 m. With increasing the rf power the current I_p ramps up and via a current jump phenomenon closed magnetic surfaces are formed [1, 2]. Relatively higher vertical field B_z was found to be required to ramp up current even in the initial phase. This has been observed in CDX-U[3] and LATE[4]. Since both extraordinary (X) and ordinary (O) waves are lunched from the low field side (LFS), they cannot access to the electron cyclotron resonance (ECR) beyond the cutoff layers (right-hand and plasma) without mode conversion to the electron Bernstein wave (B) [5, 6]. The conversion efficiency η_{XB} from X to B or transmission efficiency T_{OX} from O to X mode at the cutoff layer strongly depends on the density scale length $L_n = n_e / |\partial n_e / \partial r|$. In order to achieve high η_{XB} the short L_n of ~ 5 mm is required [7]. However, it has been well known that the steep density gradient ∇n_e drives density fluctuations in the toroidal device. Under such situations, since the conversion layer becomes rough and wavy due to fluctuations, T_{OX} is reduced at high $\tilde{n}_e/n_e$ and high poloidal wave length λ_{pol} [8]. Using a simple spectrum of the poloidal refractive index T_{OX} is calculated as a function of L_n for various $\tilde{n}_e/n_e$ as shown in Fig.1. Since $\tilde{n}_e/n_e$ > 30-40 % and wave length > 25 mm are observed in the annulus plasma, these fluctuations must be stabilized from a view point of higher mode conversion efficiency which is required to heat plasma and drive plasma current. Although both drift and flute modes driven by a steep ∇n_e with L_n= 20-60 mm have been studied in a simple torus BETA using 2.45GHz microwave, the effects of these waves on the X-B conversion have not been studied [9]. In this report we present the details of characteristics of the density fluctuations in the annulus plasma, and study the stabilization (field line tying [10] and magnetic shear [11]) effects of vertical field B_z on them in the weak mirror configuration.

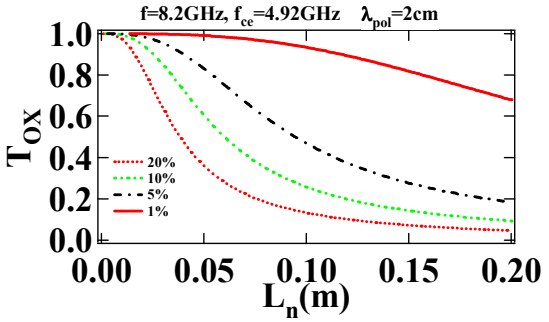

Fig.1 T_{OX} v.s. L_n at f=8.2 GHz. $\tilde{n}_e/n_e$ =1%(solid), 5%(dot-dashed), 10%(dashed), and 20%(dotted). λ_{pol} =2 cm, and parallel refractive index $N_{||}$=0.7.

2. Experimental Arrangement

2.1. CPD device and diagnostics

CPD is a spherical tokamak device whose diameter as well as height is ~ 1.2 m. The diameter of the center stack is 0.255 m. Mirror configurations (decay index ~ 0.046, B_z ~ 40 G at R=0.2 m) are used to ramp-up Ip, which is measured with the Rogowski coil installed inside the CPD chamber.

A thermal Li sheet beam is injected from the bottom of the chamber and the 2D image of LiI (670.8 nm) is used to analyze the density profile [2,12,13]. The line averaged density is measured along the vertical chord at R=0.3 m by an interferometer at 140 GHz. The scattered microwave component at the cutoff layer is monitored around the torus.

author's e-mail: ryoukai@triam.kyushu-u.ac.jp

The X-wave reflected from the cutoff layer is measured with a reflectmeter. T_e is measured by a scanning Langmür probe.

2.2. Li beam fluctuation spectroscopy (LBFS)

The LBFS system measures local, long wavelength ($k_\perp \rho_s$<1) density fluctuations by observing LiI. Fluctuations in LiI are proportional to the local density fluctuations, $\tilde{n}_e/n_e = \tilde{I}_{Li}/I_{Li}$. The radial resolution is ~ 5 mm ϕ. The LBFS system consists of 50 spatial points, connected to photomultiplier tubes via a fiber bundle. The image area is 50 mm ×25 mm. The sampling frequency of ADC is 300 kHz.

3. Measurement of Density Fluctuations

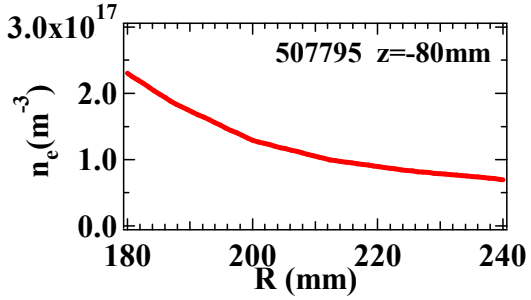

Fig.2 Density profile at z=-80 mm. R_{res}=164 mm.

3.1. Fluctuations in Annulus plasma

Characteristics of density fluctuations in initially produced annulus plasma are investigated. Since the plasma is vertically extended, the LiI intensity drops sharply for R< R_{res}, where flute modes are expected to stable due to $\vec{\nabla}n \cdot \vec{\nabla}B < 0$, but it decays gradually for R>R_{res}, where flute modes become unstable due to $\vec{\nabla}n \cdot \vec{\nabla}B > 0$ .The

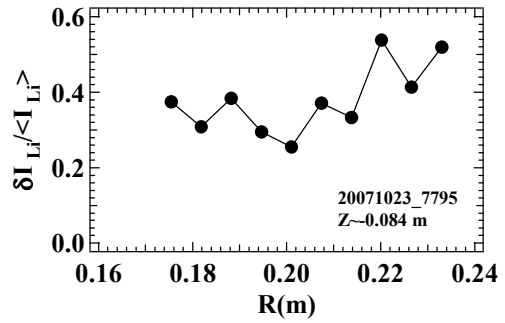

Fig.3 $\tilde{n}_e/n_e$ vs. R. Relative amplitude gradually increases along the major radius.

contour of the density aligns along the vertical direction [2] and the radial profile at Z= -80 mm, as shown in Fig.2. According to the density profile with L_n ~ 40 mm, R_{cutoff} and R_{UHR} are calculated to be 0.23 m and 0.19 m, respectively. Since this cutoff layer extends vertically, X-mode from LFS cannot access the resonance layer. Both flute and drift modes are also unstable in this region. Figure 3 shows a radial distribution of the relative

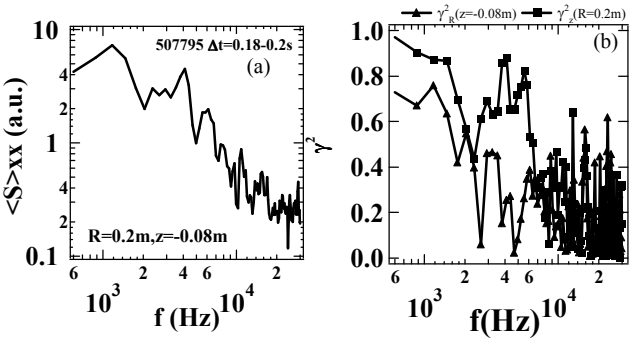

Fig.4 The auto power (a), and γ_R^2 and γ_Z^2 spectra (b).

fluctuation amplitude. The amplitude is 25-50 % around the expected mode conversion layer, which becomes rough and wavy due to fluctuations. The auto power spectrum S_{xx} and square coherency γ_R^2 (γ_Z^2) at two points separated by horizontal distance of ΔR~ 2.5 cm (vertical distance of ΔZ ~ 1.25 cm) are analyzed by fast Fourie transform FFT, as shown in Fig.4. The time window is ~ 20 ms and moving average at every 3.4 ms (1024 data

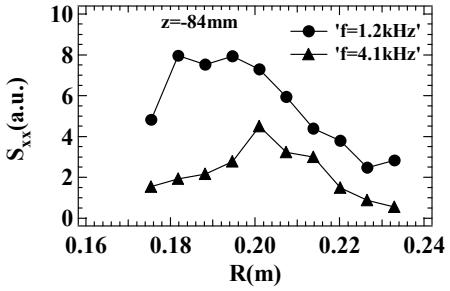

Fig.5 Radial profiles of S_{xx} at f=1.1 and 4.1 kHz.

points) is used. The frequency resolution is 0.3 kHz. S_{xx} shows a broadband spectrum peaking at f~ 1.1 kHz and decaying to ~ 10 kHz as f^{-1}. At f~ 1.1 kHz both γ_R^2 and γ_Z^2 are ≥ 0.7, but, at f = 4.1 kHz γ_R^2 is reduced < 0.3 while γ_Z^2 > 0.8. The radial profiles of S_{xx} at f=1.1 and 4.1 kHz are shown in Fig. 5. The former shows a broad peak at 0.19 m and sharply decreases in the LFS. The latter also peaks at R~ 0.2 m and decays at both sides. Figure 6 shows that a mode at f=1.1 kHz is extended coherent mode and a mode at 4.1 kHz is a relatively localized one. The radial correlation length for the 1.1 kHz mode is

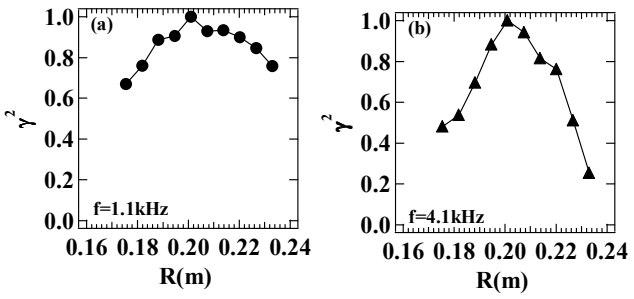

Fig.6 Radial profiles of γ_R^2 at 1.1 (a) and 4.1 kHz (b).

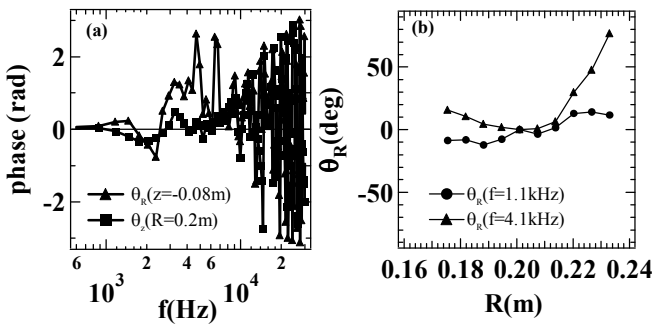

Fig.7 The cross phase θ_R and θ_Z spectra (a), radial profiles of θ_R at f=1.1 and 4.1 kHz.

considered to be longer than the viewing radial length of 0.06 m, and that for 4.1 kHz mode is < 0.03 m. However, the vertical profiles of γ_Z^2 shows a high coherence > 0.9, suggesting that both coherent modes are extended along the vertical direction. These modes are, therefore, expected to be aligned along the contour of the density. The cross phases θ_R and θ_Z at two points separated by $\Delta R \sim 2.5$ cm ($\Delta Z \sim 1.25$ cm) are also shown in Fig.7. The θ_R spectrum rapidly deviates in the lower frequency range because the mode at 4.1 kHz is localized at R~0.2 m ± 0.02 m, on the other hand θ_Z is remained around zero. These correspond to γ_R^2 and γ_Z^2spectra in Fig. 4 (b). The mode at 1.1 kHz propagates along the major radius with a phase velocity of ~ 1 km/s, as shown in Fig. 7(b). Since the variation in θ_Z is within ± 5 deg at both frequencies, the wave number k_z along the vertical direction is ~ 0.01 cm^{-1}.

3.2. Stabilization in weak mirror configuration

As mention in §1, the necessary condition for current ramp-up is pre-applied vertical field, which is relatively higher from a view point of equilibrium. The reason why this condition is required has been partially studied as the uni-directional Pfirsch-Schlüter current along the inclined

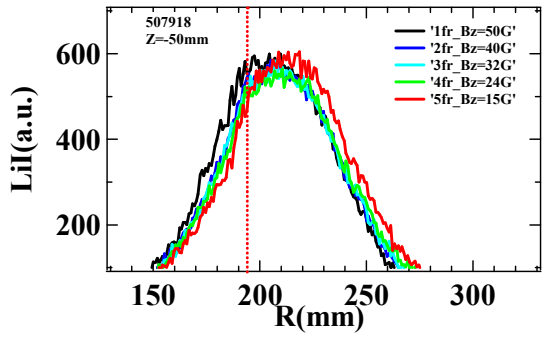

Fig.8 Radial profiles of LiI at z=-50 mm below the equator at B_z = 15-50 G. The dotted line corresponds to the resonance layer.

magnetic field or toroidal precession current due to the deeply trapped particles created by ECW[3,4]. However, the effects of density fluctuations have been never considered. In this section how the B_z affects the density fluctuations will be presented.

In Fig. 8 the radial profiles of LiI images at various B_z values, indicating that B_z (< 50 G) does not affect intensity profiles, namely the 2D structures of density. Since the effect of B_z on n_e (R,z) is insignificant, the driven force (∇ n) for the density fluctuations is also unchanged. However, it should be noted that the relative fluctuation amplitude decreases with increasing B_z, as shown in Fig. 9.

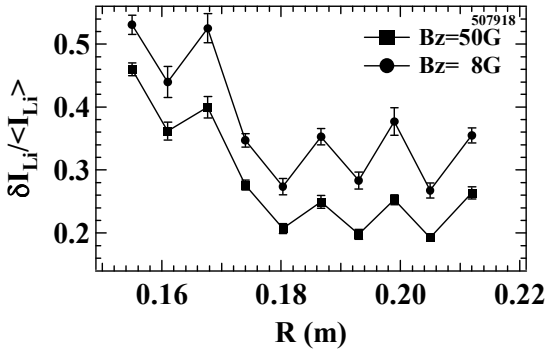

Fig. 9 $\tilde{n}_e/n_e$ vs. R. Two profiles taken at B_z=8 and 50 G are shown.

In this experiment B_z was swept in step like manner for each 30 ms. Since resonance position is R_{res}=0.19 m, the larger $\tilde{n}_e/n_e$ might be driven by the steeper density gradient for $R < R_{res}$.

Although the reduction of relative amplitude is ~ 0.8 by with B_z=50 G at B_t=0.3T, the characteristics of the fluctuations are drastically changed. Auto power and square coherency spectra are shown in Fig.10. The integrated power in the low frequency range changes by a similar factor compared with that in the relative amplitude. The coherency and its spatial structure are quite drastically

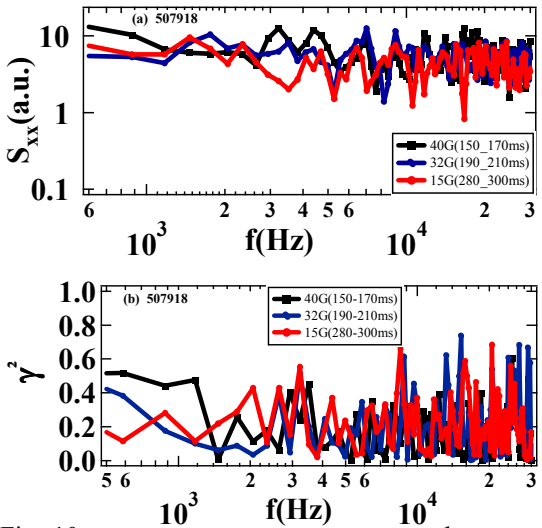

Fig. 10 The auto power (a), and square coherency γ^2 spectra (b) at various B_z.

changed. Although coherent low frequency waves are unstable at B_z=0 G, both coherencies between two horizontally and vertically separated points are much

reduced as B_z exceeds a certain value.

Figure 11 shows the stabilization effects of Bz on the

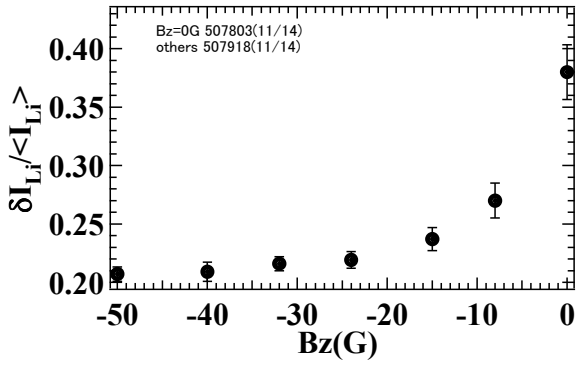

Fig. 11 Bz dependence on $\tilde{n}_e/n_e$

density fluctuation amplitude. Usually current ramp-up experiments have been done at relatively higher Bz value in a week mirror configuration. According to result in Fig. 1 this stabilization effect is considered to be necessary for better conversion efficiency to EBW.

4. Discussion

Changes in L_c and pitch angle are shown in Fig. 12. Here the connection length L_c is defined as the wall to wall length of the field lines, and pitch angle $\theta = \tan^{-1}(B_z/B_\tau)$. Since B_z is varied up to 50 G, L_c becomes shorter at higher B_z. For $R < R_{res}$ the maximum of L_c is bounded by the case at B_z=15 G and sharply decays towards the CS. On the other hand, it reduces gradually for $R > R_{res}$. In the region of interest L_c varies from 200 m to 70 m as B_z increases. Thus, stabilization effects of field line tying can be possible. Since the decay index of B_z is small and the radial variation of B_z is small, the magnetic shear length $L_s = \theta/(d\theta/dR)$, is an order of 0.2 m on the mid plane

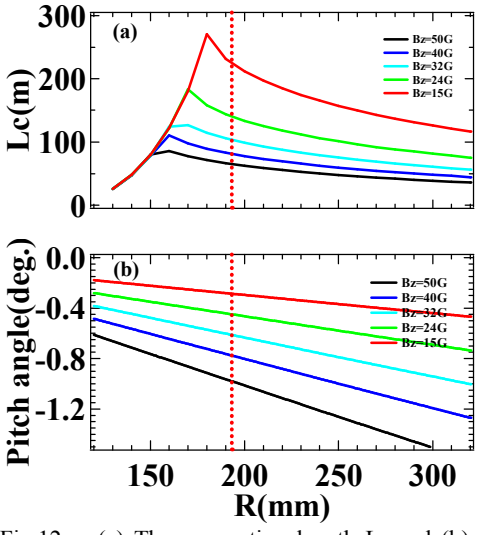

Fig.12 (a) The connection length L_c and (b) pitch angle θ_{pitch} for various B_z. The dotted line indicates the resonance layer.

at $R=R_{res}$ and it increases monotonically along R. Since L_s/L_n is an order of 5-10, the magnetic shear effects are also expected, as shown in Fig. 13.

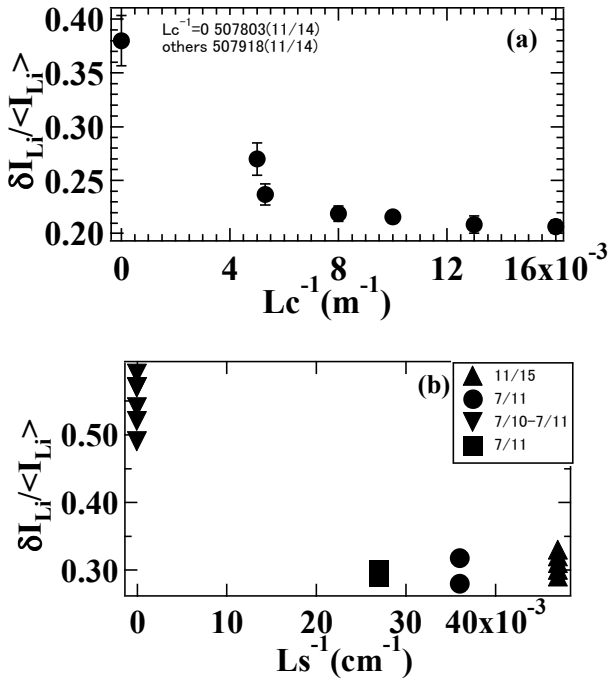

Fig. 13 The relative amplitude vs. L_c (a) and L_s (b)

5. Conclusion

The 2 D structure of density fluctuations has been measured with LBFS in annulus rf plasma which has been produced by ECR. The equi-density contour is observed to be aligned along the vertical direction and coherent waves are found to be excited in the low frequency range (1-10 kHz). It should be noted that the vertical field, which is pre-required for ramp-up plasma current, stabilizes these coherent waves. The relative amplitude is reduced by a factor of 2 and the correlation length is reduced < 5 mm. The line tying and magnetic shear effects seem to play more role in stabilization mechanisms.

References

[1] T. Yoshinaga, et al., 22nd IAEA FEC EX/W (2008)
[2] T. Kikukawa, et al., J. PFR **3**, 010 (2008)
[3] C.B.Forrest,et al., PRL 68 (1992) 3559.
[4] T. Maekawa T. et al, NF **45** (2005)1439.
[5] A. K. Ram and S. D. Schultz, POP **7**, 4084 (2000)
[6] E. Mjølhus, J. Plasma Phys. **31**, 7 (1984).
[7] S. Shiraiwa, et al., PRL **96,** 185003 (2006).
[8] H.P. Laqua, et al., PRL 78 (1997) 3467.
[9] P. K. Sharma et al., PPCF **39** (1997) 1669.
[10] F.F. Chen et al., Phys. of Fluid 8 (1965) 912.
[11] F.F. Chen et al., PRL **18** (1967) 639.
[12] H. Zushi, et al, J. Nucl. Mater. **363**, 1429 (2007)
[13] R.Bhattacharyay, et al, POP **15**, 022504 (2008)